Front. Environ. Sci. Eng. 2017, 11(2): 15
DOI 10.1007/s11783-017-0921-y

RESEARCH ARTICLE

Performance and mechanism for cadmium and lead adsorption from water and soil by corn straw biochar

Tong Chi, Jiane Zuo (✉), Fenglin Liu

State Key Joint Laboratory of Environment Simulation and Pollution Control, School of Environment, Tsinghua University, Beijing 100084, China

HIGHLIGHTS

- Corn straw biochar prepared under 400 °C has the best Cd and Pb adsorption capacity
- Maximum adsorption capacity of Cd and Pb were 43.48 and 22.73 mg·g^{-1}, respectively
- The dominant mechanism of Cd and Pb adsorption was precipitation
- Biochar could reduce the bioavailability of heavy metals when mixed with soil

GRAPHIC ABSTRACT

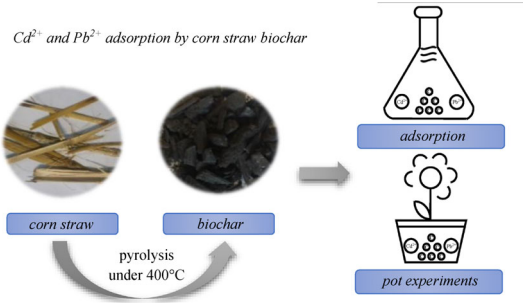

ARTICLE INFO

Article history:
Received 16 October 2016
Received in revised form 7 January 2017
Accepted 1 March 2017

Keywords:
Corn straw
Biochar
Heavy metals
Sorption isotherm
Bioavailability

ABSTRACT

Cadmium (Cd) and lead (Pb) in water and soil could be adsorbed by biochar produced from corn straw. Biochar pyrolyzed under 400°C for 2 h could reach the ideal removal efficiencies (99.24% and 98.62% for Cd and Pb, respectively) from water with the biochar dosage of 20 g·L^{-1} and initial concentration of 20 mg·L^{-1}. The pH value of 4–7 was the optimal range for adsorption reaction. The adsorption mechanism was discussed on the basis of a range of characterizations, including X-ray diffraction (XRD), X-ray photoelectron spectroscopy (XPS), Fourier transform infrared spectroscopy (FTIR) and Raman analysis; it was concluded as surface complexation with active sorption sites (-OH, -COO-), coordination with π electrons (C = C, C = O) and precipitation with inorganic anions (OH^-, CO_3^{2-}, SO_4^{2-}) for both Cd and Pb. The sorption isotherms fit Langmuir model better than Freundlich model, and the saturated sorption capacities for Cd and Pb were 38.91 mg·g^{-1} and 28.99 mg·g^{-1}, respectively. When mixed with soil, biochar could effectively increase alkalinity and reduce bioavailability of heavy metals. Thus, biochar derived from corn straw would be a green material for both removal of heavy metals and amelioration of soil.

1 Introduction

Pollution of heavy metals in water and soil is a serious problem all over the world. In recent years, with the aggravation of human activities such as mining, smelting, processing industry and commercial manufacturing, a lot of heavy metals such as cadmium, lead, mercury, cobalt, etc. are discharged into atmosphere, water and soil causing serious environmental pollution [1]. Cadmium and lead are two of the most common heavy metals with high toxicity and carcinogenicity.

Chemical precipitation, lime coagulation, ion exchange, membrane separation and advanced oxidation processes are common technologies for removing heavy metals, which however, are expensive and not environmental friendly in many cases. Hence, reports about employing adsorbents derived from agricultural waste to remove heavy metals have caught more and more attention. Velazquez-Jimenez et al. [2] demonstrated that agave

✉ Corresponding author
E-mail: jiane.zuo@tsinghua.edu.cn

bagasse presented outstanding removal capacity for Cd(II), Pb(II) and Zn(II) ions. *Lemna perpusilla* Torr, a dried aquatic plant, was proved to be a good adsorbent for Pb(II), and the maximum adsorption efficiency was above 95% after 210 min with a dose of 4 $g \cdot L^{-1}$ and an initial Pb(II) concentration of 50 $mg \cdot L^{-1}$ [3].

Besides raw agricultural waste, some adsorbent materials prepared from agricultural waste can also remove these heavy metals from contaminated water and soil efficiently. One of these materials is biochar [4], which is carbon-enriched and porous material produced from pyrolysis process of biomass under anaerobic condition. Biochar derived from switch grass could remove Cd(II) and Cu(II), and the sorption capacities of biochar for Cd(II) and Cu(II) were 34 and 31 $mg \cdot g^{-1}$, respectively [5]. Giant miscanthus biochar could remove Cd(II), and the sorption capacity was up to 13.24 $mg \cdot g^{-1}$ with pyrolysis temperatures higher than 500°C [6]. Meanwhile, Yuan et al. confirmed that the pH value of biochar derived from straws increased as the pyrolysis temperature increased from 300°C to 700°C and showed alkalinity [7]. Thus, biochar can be used as soil amendment to increase soil alkalinity, improve soil fertility, change microbial community structure and enhance plant growth [8]. It can also retain pollutants in soil, especially heavy metals [9]. Bian et al. found that Cd and Pb was immobilized in soil mixed with wheat straw biochar, and the concentration of heavy metals was significantly reduced in rice plant tissues [10]. Rice straw biochar could reduce the concentration of Cu and Pb in the shoots of *Sedum plumbizincicola* by 46% and 71%, respectively [11].

Corn is one of the principal food crops, and the yield of corn straw is more than 200 million t/a in China. At present, the major disposal method of corn straw is incineration, during which large amounts of CO_2 (more than 10 million t/a) [12], CO, $PM_{2.5}$ and black carbon are discharged into the atmosphere, causing serious air pollution [13]. Thus, disposing corn straw through anaerobic pyrolysis to produce biochar as soil amendment and heavy metals adsorbent can achieve the goal of resource and energy recycling, while avoiding the severe air pollution caused by incineration. Besides, compared to other efficient and widely used adsorbents such as activated carbon, lower price due to cheap or no expense of raw materials makes biochar more competitive [14]. Furthermore, application of biochar in farmland was proved to be useful for reducing the emission of N_2O, which is a dominant ozone-depleting substance as well as a potent greenhouse gas [15]. And because of its heterogeneous chemical nature and particular form, biochar can resist extreme climate [16] and persist longer in the soil than other forms of organic carbon. Therefore, biochar is regarded as a sink of carbon and can efficiently avoid contribution to CO_2 emission and mitigate climate change [17].

The objective of this study is to manufacture biochar under different pyrolysis temperatures using corn straw, explore the mechanism of adsorption of Cd and Pb, and study the influence of biochar on plant growth and bioavailability of Cd and Pb in soil.

2 Materials and methods

2.1 Preparation of Biochar

The raw corn straw was taken from Xichuan county in Henan Province, China. The straw was first broken into pieces, put into sealed iron container and then burnt in muffle furnace for 2 h under different temperatures of 200°C, 300°C, 400°C, 500°C, 600°C and 700°C, and the products were hence called as B200, B300, B400, B500, B600 and B700, respectively. Finally, the biochar was pulverized into powers to pass through a screen of 60 meshes.

2.2 Cd and Pb adsorption experiments

Cd and Pb stock solution (1000 $mg \cdot L^{-1}$) were prepared by dissolving 2.103 g cadmium nitrate ($Cd(NO_3)_2$, Sinopharm Chemical Reagent) and 1.599 g lead nitrate ($Pb(NO_3)_2$, Sinopharm Chemical Reagent) into deionized water in 1000 mL volumetric flasks. The pH value of stock solution was adjusted to be acidic by adding 0.1 mL of Nitric acid (HNO_3, 63 wt.%), respectively. The two kinds of stock solution were diluted into 20 $mg \cdot L^{-1}$ before adsorption experiment, so that the pH value increased to 4.5±0.5, which eliminated the effect of precipitation of metals. Diluted solution (50 mL) and biochar (1 g) were put into a 250 mL conical flask, and then shaken in table rotary shaker (146 $r \cdot min^{-1}$) at 25°C. After 60 min, 1-2 mL liquid was taken out and filtered with 0.45 μm membrane filters, and the concentrations of Cd and Pb were then measured by inductive coupled plasma atomic emission spectrometer (ICP-AES, Thermo Fisher Scientific, America).

To simulate the sorption isotherm of Cd and Pb, Langmuir (Eq. (1)) and Freundlich (Eq. (2)) models were used to fit the data.

$$q = \frac{bq^0 Ce}{1 + bCe}, \tag{1}$$

$$q = KCe^{1/n}, \tag{2}$$

where, q ($mg \cdot g^{-1}$) is the equilibrium adsorbed concentration of Cd and Pb and Ce ($mg \cdot L^{-1}$) is the equilibrium concentration of solution. In the Langmuir model, q^0 ($mg \cdot g^{-1}$) denotes the maximum sorption capacity, while b ($L \cdot mg^{-1}$) represents binding energies. In the Freunlich model, K ($[mg \cdot g^{-1}]/[mg \cdot L^{-1}]^{-1/n}$) is affinity coefficient, and

n is a non-dimensional constant indicating the Freunlich linearity.

2.3 Pot experiment

Soil was taken from Xichuan County, China. Plain soil and soil-biochar mixture with ratios of 2.5, 5, 10 wt.% were prepared. To evaluate influences of biochar on pH value of soil, 5 g of the soil sample was taken after 5, 100, 200, 400, 600, 800 and 1200 h. According to ISO 10390: 2005, all the samples were air-dried and crushed into fine particles with diameter less than 2 mm. After that, 2.5 g treated sample was added into 25 mL of 0.01 mol·L^{-1} $CaCl_2$ solution and shaken for 2 h. After still standing for 1 h, the pH value of supernatant liquor was measured as the pH value of the soil or soil-biochar mixture. As a common plant in China of which the height and the number of sprouts were easy to measure, *Ligustrun lucidum* was planted in soil and soil-biochar mixture to explore the facilitation of biochar to plant growth. To begin with, all plants were clipped to the same height (40 cm) and the sprouts were picked off. In the next two months, the height of each plant was measured every 3–5 days. And the date when first sprout came out was recorded.

To investigate the bioavailability of Cd and Pb in soil and biochar-soil mixture, a pot experiment was carried out. $Pb(NO_3)_2$ and $Cd(NO_3)_2$ solution were added into soil, respectively, and the initial concentration were 30 mg-Cd/kg-soil and 1500 mg-Pb/kg-soil. Twenty seeds of *Selaginella uncinata* were sown into each porcelain pot. After three months, roots and leaves were taken and dried at 60°C for 72 h. After weighed and crushed, the samples were treated by tri-acid solution. The concentrations of Cd and Pb in roots and leaves were analyzed by ICP-AES. All the samples were taken in triplicate during the experiment.

2.4 Characterization

X-ray diffraction (XRD, D8 ADVANCE, Bruker Corporation, Massachusetts, USA) patterns were used to investigate the mineral composition of biochar. The Cu-Kα radioactive source was high-power with generator tension being 40 kV and current being 40 mA. Collected sequential scans were at a rate of 6° min^{-1} of 2θ from 10° to 80°. JADE 5.0 software (Jade Software Corporation, Christchurch, New Zealand) was used to analyze the XRD patterns. X-ray photoelectron spectroscopy (XPS, ESCALAB 250Xi, Thermo, UK) was used to characterize the valence state of element and the surface composition. Fourier Transform infrared spectroscopy (FTIR) spectra detection was carried out with Nicolet 6700 (Thermo Corp., USA). Before measurement, 1 wt.% sample was mixed with 100 mg KBr powder and the mixture was pressed into a transparent sheet. The average over 9 scans was collected for each measurement with scan range varying from 4000 cm^{-1} to 400 cm^{-1} and the resolution was 4 cm^{-1}. Raman microspectrometer (Renishaw Research Raman Microscope System RM2000, UK) was used to detect the Raman scattering and Raman-imaging of biochar.

3 Results and discussion

3.1 Cd and Pb adsorption on biochar

The removal efficiencies of Cd and Pb after 60 min by biochar prepared at different pyrolysis temperatures were shown in Fig. 1. As pyrolysis temperature increased, the removal efficiency increased as well for both Cd and Pb. The removal efficiencies of Cd and Pb by biochar could achieve 98% and 99%, respectively, when the pyrolysis temperature was above 400°C. Considering the removal efficiency and the energy consumption, B400 was determined as the suitable biochar for adsorbing Cd and Pb from contaminated water.

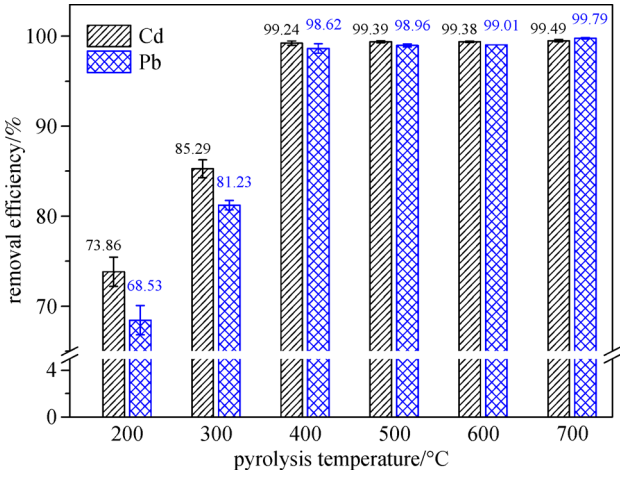

Fig. 1 Removal efficiencies of Cd and Pb adsorbed by biochar prepared under different pyrolysis temperature. Initial concentration of both Cd and Pb solution was 20 mg·L^{-1}; reacting temperature was 25℃; dosage of biochar was 20 g·L^{-1}

As Cd^{2+} and Pb^{2+} will precipitate with OH^- when the alkalinity of solution increased, the influence of pH value on removal efficiency was evaluated. Nitric acid (HNO_3, 63 wt.%) and sodium hydroxide (NaOH, 40 wt.%) were used to adjust and maintain the pH value at 1, 4, 7, 10 and 13. For Cd adsorption, no precipitation was formed at pH = 1 and only 1.52% Cd was removed by biochar (Fig. 2(a)). Regmi et al. got similar results at pH = 2 and attributed this appearance to the inhibition effect of H^+ on reaction between oxygen containing functional groups and metal ions [5]. Iqbal et al. believed that anion groups on the surface of adsorbents which were active sorption sites reacting with Cd^{2+} and Pb^{2+}, would be occupied by H^+ of high concentration and become protonated, losing the function of binding with metals [18,19]. Removal

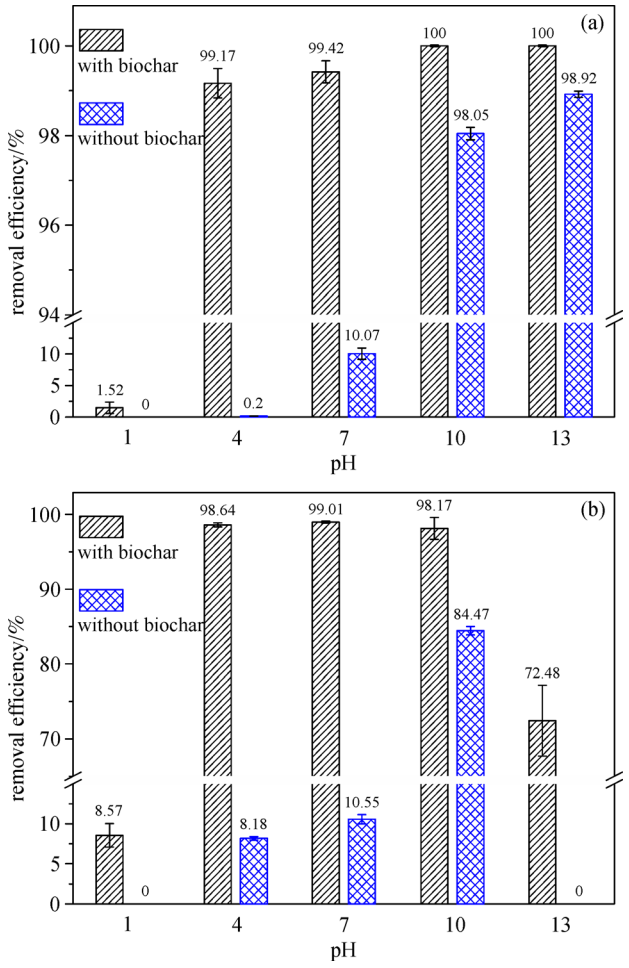

Fig. 2 Removal efficiency of (a) Cd and (b) Pb with or without biochar under different pH value. Initial concentration of both Cd and Pb solution was 20 $mg \cdot L^{-1}$; reacting temperature was 25ºC; dosage of biochar was 20 $g \cdot L^{-1}$

efficiency with biochar under slightly acidic condition (pH = 4) was as high as neutral condition (pH = 7), both exceeding 99%. When pH increased to 7, 10.07% Cd was removed through precipitation without biochar adsorption, which could be corroborated by the research of Kim et al. (4.6%, initial concentration = 10 $mg \cdot L^{-1}$, pH = 6) [6]. However, after adding biochar, removal efficiency increased to just 13% in their study, much lower than this study. When pH value was higher than 10, little Cd in the aqueous solution could be detected due to the precipitation, indicating that most Cd was removed through surface precipitation mechanism under alkaline conditions.

Similarly, efficiency of Pb removal with or without biochar changed in the same way with Cd under pH = 1–10 (Fig. 2(b)). However, as alkalinity increased, the precipitation $Pb(OH)_2$ began to dissolve into plumbates(II) ($[Pb(OH)_3]^-$), and no precipitation exists under pH = 13. With the presence of biochar, 72.48% of Pb (mostly exists as $[Pb(OH)_3]^-$) was removed due to the adsorption function of biochar. Compared to that under pH 4–10, the lower removal efficiency might be ascribed to the dissolution of precipitation $Pb(OH)_2$, weaker ability of adsorbing Pb-containing anion (namely plumbates(II), $[Pb(OH)_3]^-$) of our sorbent or the competition between OH^- and $[Pb(OH)_3]^-$ when complexing or coordinating with some certain functional groups.

3.2 Characterization

3.2.1 X-ray diffraction characterization

The XRD patterns of biochar before and after adsorption of Cd and Pb were as shown in Fig. S1(see supplementary material). On all of the three curves, peaks of sylvine (KCl, JCPDS 75-0296) at $2\theta = 28.347°$, 40.520°, 50.188° for (2 0 0), (2 2 0), (2 2 2) reflections could be detected. The reduction of sylvine peaks for Cd- and Pb-adsorbed biochar indicated that K^+ released due to electrostatic cation exchange with Cd^{2+} or Pb^{2+} [20]. The wide diffraction peak at $2\theta \approx 24°$ corresponded to amorphous silica [21], which was a little unconspicuous on Cd- and Pb-adsorbed biochar owing to peaks of otavite and susannite at contiguous degree. After biochar adsorbing Cd, peaks at $2\theta = 30.275°$, 23.485°, 49.908° assigned to (1 0 4), (0 1 2), (1 1 6) reflections indicated the formation of otavite ($CdCO_3$, JCPDS 42-1342). Thus the mechanism of Cd removal by biochar can be proposed as Eq. (3), which was consistent with the deduction of Xu et al. [22]. After biochar adsorbing Pb, a new crystalline phase, susannite ($Pb_4SO_4(CO_3)_2(OH)_2$, (JCPDS 89-7549), was detected through the diffraction peaks at $2\theta = 24.924°$, 34.211°, 30.397° for (1 1 –2), (3 0 0), (1 1 –3) reflections, respectively. Same substance was found in the research of Wang et al. [23]. The mechanism can be described as Eq. (4), in which the anions (SO_4^{2-}, CO_3^{2-}, OH^-) might be released from dissolved minerals in straw. Expect for sylvine, otavite and susannite, no obvious peaks of other substances were observed, indicating that CO_3^{2-}, SO_4^{2-} and OH^- were crucial inorganic function groups for mineral precipitation process by corn straw derived biochar.

$$Cd^{2+} + CO_3^{2-} = CdCO_3 \downarrow \quad (3)$$

$$4Pb^{2+} + 2CO_3^{2-} + SO_4^{2-} + 2OH^- = Pb_4SO_4(CO_3)_2(OH)_2 \downarrow \quad (4)$$

3.2.2 X-ray photoelectron spectroscopy characterization

To get further information about the reaction process, XPS technique was employed. For all peaks, C1s binding

energy at 284.8 eV was used as calibration as shown in Fig. S2(a). After adsorption of Cd and Pb, this peak at 284.8 eV attributed to C-C/C-H bonds did not shift, so we could infer that carbon existed as C-C/C-H might not take part in the adsorbing reaction. The peak at 286.4 eV on straw standing for C-O bond [24,25] disappeared on curves of biochar, which indicated that pyrolysis process made C-O fractured. The O1s peaks for Cd- and Pb-adsorbed biochar were both decomposed into two peaks, as shown in Fig. S2(b). For Pb-adsorbed biochar, the peak at 531.8 eV reflected the interaction between Pb^{2+} and O^{2-} [26]. For Cd-adsorbed biochar, the peak at 531.4 eV represented O^{2-} in cadmium carbonate [27], which corresponded to the results of XRD patterns. The peak at 532.8 eV on straw was due to C = O compound key. On biochar curve, this peak shifted to 531.7 eV which attributed to O-H or C-O-N compound keys, indicating that C = O bond ruptured after pyrolysis. The peaks for adsorbed biochar near 532.8 eV might be a result of the re-formation of C = O bond during the adsorption. As shown in Fig. S2(c), peaks at 412.7 and 405.9 eV representing Cd3d could perfectly inosculate with the binding energy of $CdCO_3$ [28]. For Pb-adsorbed biochar, the peak at 139.2 eV in Fig. S2(d) probably stood for the reciprocity among OH^-, CO_3^{2-}, SO_4^{2-} groups and Pb^{2+} according to the XRD patterns.

3.2.3 Fourier transform infrared spectroscopy characterization

The FTIR spectroscopy as shown in Fig. S3 could illustrate the function group of biochar before and after adsorption of Cd and Pb. The obvious and wide peak around 3430 cm^{-1} represented O-H vibrations of hydroxyl function groups in phenols, carboxylic acids or other polymeric compounds, which was a common FTIR peak for biomass materials [29,30]. For the raw straw, peaks at 2916 and 1735 cm^{-1} were corresponded to C-H vibration of aliphatic CH_2 unit and C = O bond of carboxyl groups, respectively [18]. These two peaks disappeared on the curve of biochar because of pyrolysis process. Nevertheless, for adsorbed biochar, the two peaks were observed again due to surface complexation and metal π-interaction mechanisms [23]. The peak at 1638 cm^{-1} indicating C = C/C = O for straw shifted to 1585 cm^{-1} for biochar, and then shifted to 1597/1593 cm^{-1} after adsorption of Cd and Pb, respectively. The peak at 1394 cm^{-1} representing -COO- shifted to 1381/1383 cm^{-1} after adsorption of Cd and Pb, respectively. Thus we can infer that π electrons of C = C and C = O took part in the metal ion uptake. The peak of CO_3^{2-} at 1431/1431 cm^{-1} on adsorbed biochar convincingly demonstrated the precipitation between Cd^{2+}/Pb^{2+} and CO_3^{2-} [4,22]. The peak at 1050 cm^{-1} indicated that C-O bond on straw disappeared after pyrolysis [31], in accordance with inference of XPS characterization.

3.2.4 Raman spectrum characterization

Raman spectra of biochar before and after adsorption of Cd and Pb in the wavelength region of 1000–2000 cm^{-1} were shown in Fig. S4. Peaks at 1368–1384 cm^{-1} and 1588–1600 cm^{-1} were in accord with D and G bands, respectively. The changes of G bands after adsorption, which indicated sp2 carbon, could be attributed to π electrons interaction mechanisms. D bands were much weaker than G bands, demonstrating little disorder of carbon atoms [29].

From the XPS, FTIR, Raman and XRD analysis, it could be concluded that Cd and Pb had been adsorbed by biochar. Mechanisms of surface complexation with active sorption sites (-OH, -COO-), coordination with π electrons (C = C, C = O) and precipitation with inorganic anions (OH^-, CO_3^{2-}, SO_4^{2-}) for both Cd and Pb were all observed in this study, among which precipitations of $CdCO_3$ and $Pb_4SO_4(CO_3)_2(OH)_2$ were the predominant contributor of adsorption.

3.3 The sorption isotherms

The initial concentration of Cd and Pb both ranged from 5 to 50 $mg \cdot L^{-1}$. To maintain Ce/C0 at 20%–80%, 0.1 g biochar was added into 100 mL solution [23]. The sorption isotherms and sorption models of Cd and Pb and the calculated sorption constants for Freundlich and Langmuir isotherm models are shown in Fig. 3. We could find that the data of both Cd and Pb fitted Langmuir model better with the correlation coefficients R^2 of 0.992 and 0.994, respectively. However, Freundlich model could also fit well and the correlation coefficients were 0.928 and 0.978. It could be inferred that biochar was a favorable adsorbent as $n>1$ ($1/n<1$) [31]. Moreover, the adsorption process tended to be monolayer adsorption, indicating the process of chemisorption [32].

According to the Langmuir model, maximum sorption capacities (q^0) were 38.91 and 28.99 $mg \cdot g^{-1}$ for adsorption of Pb and Cd, which were comparable or even higher than some other adsorbents. The comparison among adsorbents of Cd and Pb reported in literature are listed in Table 1. Although the sorption capacity of straw biochar in our research was not as high as some other adsorbents, the ability of adsorbing Cd and Pb synchronously, the cheap price and easy access of raw material make it a satisfactory adsorbent.

3.4 Influences of biochar on soil and plant growth

Compared to plain soil, the pH value of soil-biochar mixture increased significantly as biochar was mixed into soil (Fig. S5). Functional groups such as COO^- and OH^- were among the primary causes of alkalinity due to their reaction with H^+ [7].

Table 1 Comparison among adsorbents of Cd and Pb reported in literature

adsorbents	maximum sorption capacity		references
	Cd/(mg·g^{-1})	Pb/(mg·g^{-1})	
dairy manure biochar	-	140.8	[4]
Polygonum orientale Linn	-	98.39	[31]
Chinese medicine material residue biochar	-	82.5	[23]
peanut shell biochar	-	52.8	[23]
dairy manure biochar	51.4	-	[22]
Geodae-Uksae 1 stalks biochar	13.24	-	[6]
mango peel waste	68.92	99.05	[18]
peanut hull biochar	6.36	50.05	[33]
banana peels	5.71	2.18	[34]
cron straw biochar	38.91	28.99	this study

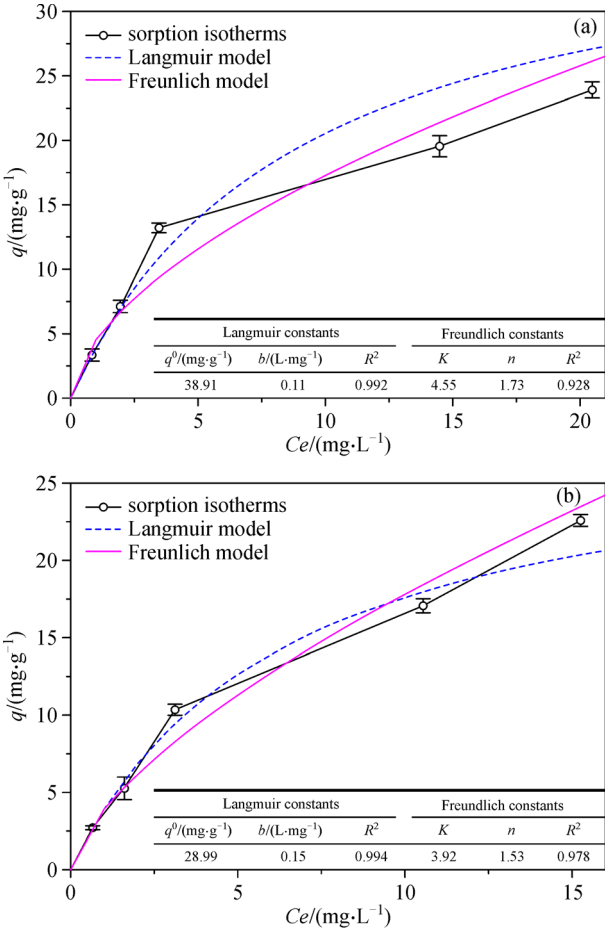

Fig. 3 The sorption isotherms and sorption models of (a) Cd and (b) Pb

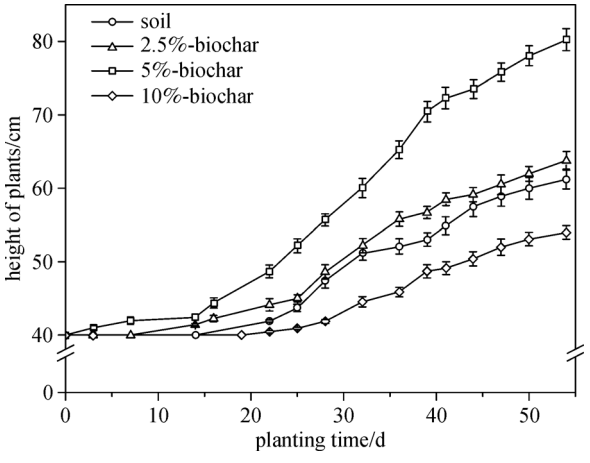

Fig. 4 Height of *Ligustrun lucidum* planted in soil amended with different ratios of biochar

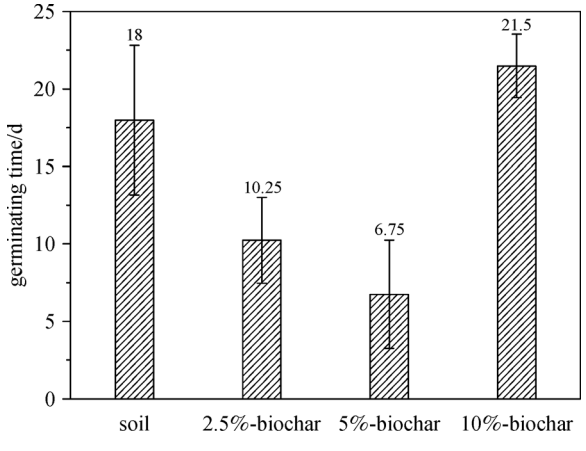

Fig. 5 Germinating time of *Ligustrun lucidum* planted in soil amended with different ratios of biochar

The acceleration of plant growth was obvious when mixing ratio was 5% as shown in Fig. 4 and Fig. 5. The height of plants increased by 40% and germination was much earlier compared to *Ligustrun lucidum* planted in plain soil. Soil-2.5% biochar mixture could also promote plant growth to a lesser extent. However, when mixing ratio was 10%, both plant growth and sprouting were suppressed, possibly because the property of soil such as

pH value was modified unduly for *Ligustrun lucidum* growth. Thus, mixing biochar into soil with appropriate proportion could efficaciously promote the growth and germination of plants.

Selaginella uncinata was used as a valuable tool for bioavailability assessment. Compared to the blank, the heavy metals concentration in roots and leaves of *Selaginella uncinata* planted in soil-biochar mixture decreased significantly as shown in Fig. 6. 10%-biochar mixture could reduce more than 70% of Cd and Pb in roots and 80% of Cd and Pb in leaves, which reflected that biochar could efficiently reduce the heavy metal bioavailability and prevent Cd and Pb from migrating into the plants.

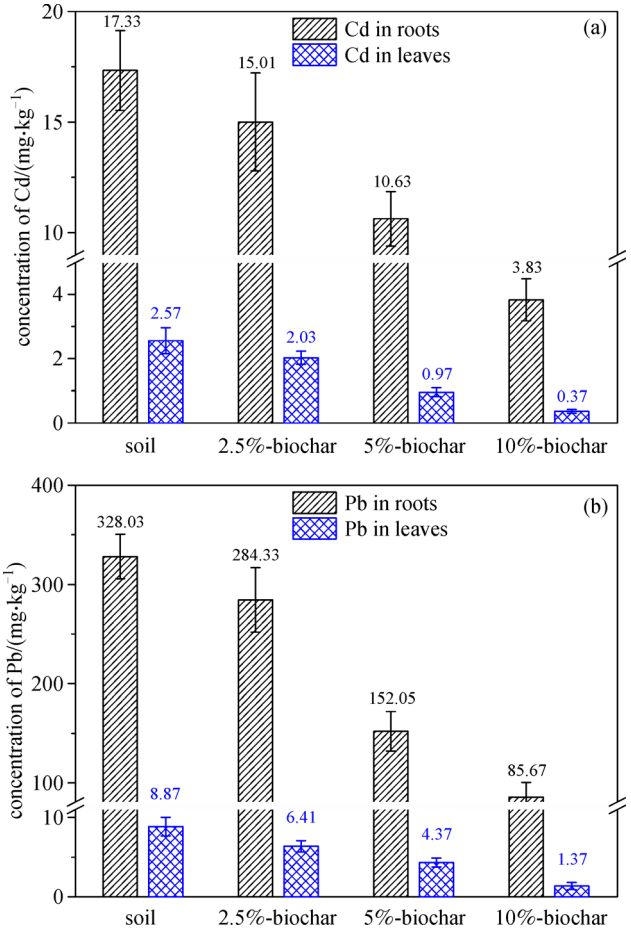

Fig. 6 Concentration of (a) Cd and (b) Pb in roots and leaves of *Selaginella uncinata*

4 Conclusions

Corn straw biochar pyrolyzed above 400°C could efficiently adsorb Cd and Pb from aqueous solution. The adsorption mechanisms of Cd and Pb were inferred to be consistent, according to the similar results of characterization and sorption isotherm tests. Mineral precipitation was the primary contributor to the adsorption process, and the precipitations were $CdCO_3$ and $Pb_4SO_4(CO_3)_2(OH)_2$, respectively. Surface complexation and π electrons interaction mechanisms were also demonstrated by characterization of FTIR, Raman and adsorption under different pH value. Mixing biochar into soil could increase the alkalinity of soil and prevent Cd and Pb from migrating into the plants.

Acknowledgements This research was financially supported by the Major Science and Technology Programs for Water Pollution Control and Management of China (Nos. 2011ZX07301-002 and 2012ZX07205-001).

Electronic Supplementary Material Supplementary material is available in the online version of this article at http://dx.doi.org/10.1007/s11783-017-0921-y and is accessible for authorized users.

References

1. Li N, Kang Y, Pan W, Zeng L, Zhang Q, Luo J. Concentration and transportation of heavy metals in vegetables and risk assessment of human exposure to bioaccessible heavy metals in soil near a waste-incinerator site, South China. Science of the Total Environment, 2015, 521-522: 144–151
2. Velazquez-Jimenez L H, Pavlick A, Rangel-Mendez J R. Chemical characterization of raw and treated agave bagasse and its potential as adsorbent of metal cations from water. Industrial Crops and Products, 2013, 43: 200–206
3. Tang Y, Chen L, Wei X, Yao Q, Li T. Removal of lead ions from aqueous solution by the dried aquatic plant, *Lemna perpusilla* Torr. Journal of Hazardous Materials, 2013, 244-245: 603–612
4. Cao X, Ma L, Gao B, Harris W. Dairy-manure derived biochar effectively sorbs lead and atrazine. Environmental Science & Technology, 2009, 43(9): 3285–3291
5. Regmi P, Garcia Moscoso J L, Kumar S, Cao X, Mao J, Schafran G. Removal of copper and cadmium from aqueous solution using switchgrass biochar produced via hydrothermal carbonization process. Journal of Environmental Management, 2012, 109: 61–69
6. Kim W K, Shim T, Kim Y S, Hyun S, Ryu C, Park Y K, Jung J. Characterization of cadmium removal from aqueous solution by biochar produced from a giant *Miscanthus* at different pyrolytic temperatures. Bioresource Technology, 2013, 138: 266–270
7. Yuan J H, Xu R K, Zhang H. The forms of alkalis in the biochar produced from crop residues at different temperatures. Bioresource Technology, 2011, 102(3): 3488–3497
8. Gul S, Whalen J K, Thomas B W, Sachdeva V, Deng H Y. Physico-chemical properties and microbial responses in biochar-amended soils: mechanisms and future directions. Agriculture, Ecosystems & Environment, 2015, 206: 46–59
9. Beesley L, Marmiroli M. The immobilisation and retention of soluble arsenic, cadmium and zinc by biochar. Environmental Pollution, 2011, 159(2): 474–480
10. Bian R, Joseph S, Cui L, Pan G, Li L, Liu X, Zhang A, Rutlidge H, Wong S, Chia C, Marjo C, Gong B, Munroe P, Donne S. A three-year experiment confirms continuous immobilization of cadmium and lead in contaminated paddy field with biochar amendment. Journal of Hazardous Materials, 2014, 272: 121–128

11. Lu K P, Yang X, Shen J J, Robinson B, Huang H G, Liu D, Bolan N, Pei J C, Wang H L. Effect of bamboo and rice straw biochars on the bioavailability of Cd, Cu, Pb and Zn to *Sedum plumbizincicola.* Agriculture, Ecosystems & Environment, 2014, 191: 124–132
12. Zhao J, Zhang G, Yang D. Estimation of carbon emission from burning of grain crop residues in China. Journal of Agro-Environment Science, 2011, 30(4): 812–816
13. Shi T T, Liu Y Q, Zhang L B, Hao L, Gao Z Q. Burning in agricultural landscapes: an emerging natural and human issue in China. Landscape Ecology, 2014, 29(10): 1785–1798
14. Rosales E, Ferreira L, Sanromán M Á, Tavares T, Pazos M. Enhanced selective metal adsorption on optimised agroforestry waste mixtures. Bioresource Technology, 2015, 182: 41–49
15. Bian R J, Chen D, Liu X Y, Cui L Q, Li L Q, Pan G X, Xie D, Zheng J W, Zhang X H, Zheng J F, Chang A. Biochar soil amendment as a solution to prevent Cd-tainted rice from China: results from a cross-site field experiment. Ecological Engineering, 2013, 58: 378–383
16. Sombroek W, Ruivo M D, Fearnside P M, Glaser B, Lehmann J. Amazonian Dark Earths as carbon stores and sinks, In: Lehmann J, Kern D C, Glaser B, Woods W I, eds. Amazonian Dark Earths: Origin, Properties, Management. Dordrecht: Kluwer Academic Publishers, 2004
17. Lehmann J. Bio-energy in the black. Frontiers in Ecology and the Environment, 2007, 5(7): 381–387
18. Iqbal M, Saeed A, Zafar S I. FTIR spectrophotometry, kinetics and adsorption isotherms modeling, ion exchange, and EDX analysis for understanding the mechanism of Cd^{2+} and Pb^{2+} removal by mango peel waste. Journal of Hazardous Materials, 2009, 164(1): 161–171
19. Saeed A, Iqbal M, Akhtar M W. Removal and recovery of lead(II) from single and multimetal (Cd, Cu, Ni, Zn) solutions by crop milling waste (black gram husk). Journal of Hazardous Materials, 2005, 117(1): 65–73
20. Lu H, Zhang W, Yang Y, Huang X, Wang S, Qiu R. Relative distribution of Pb^{2+} sorption mechanisms by sludge-derived biochar. Water Research, 2012, 46(3): 854–862
21. Yan F, Jiang J G, Chen X J, Tian S C, Li K M. Synthesis and characterization of silica nanoparticles preparing by low-temperature vapor-phase hydrolysis of $SiCl_4$. Industrial & Engineering Chemistry Research, 2014, 53(30): 11884–11890
22. Xu X, Cao X, Zhao L, Wang H, Yu H, Gao B. Removal of Cu, Zn, and Cd from aqueous solutions by the dairy manure-derived biochar. Environmental Science and Pollution Research International, 2013, 20(1): 358–368
23. Wang Z, Liu G, Zheng H, Li F, Ngo H H, Guo W, Liu C, Chen L, Xing B. Investigating the mechanisms of biochar's removal of lead from solution. Bioresource Technology, 2015, 177: 308–317
24. Singh B, Fang Y Y, Cowie B C C, Thomsen L. NEXAFS and XPS characterisation of carbon functional groups of fresh and aged biochars. Organic Geochemistry, 2014, 77: 1–10
25. Merel P, Tabbal M, Chaker M, Moisa S, Margot J. Direct evaluation of the sp^3 content in diamond-like-carbon films by XPS. Applied Surface Science, 1998, 136(1–2): 105–110
26. Lin Y Y, Liu Q, Tang T A, Yao X. XPS analysis of $Pb(Zr_{0.52}Ti_{0.48})O_3$ thin film after dry-etching by CHF_3 plasma. Applied Surface Science, 2000, 165(1): 34–37
27. Hammond A L. Geothermal resources—New look. Science, 1975, 190(4212): 370–370
28. Huang P, Zhang X, Wei J M, Pan J Q, Sheng Y Z, Feng B X. The preparation, characterization and optical properties of $Cd_2V_2O_7$ and $CdCO_3$ compounds. Materials Chemistry and Physics, 2014, 147 (3): 996–1002
29. Chia C H, Gong B, Joseph S D, Marjo C E, Munroe P, Rich A M. Imaging of mineral-enriched biochar by FTIR, Raman and SEM-EDX. Vibrational Spectroscopy, 2012, 62: 248–257
30. Liu F L, Zuo J E, Chi T, Wang P, Yang B. Removing phosphorus from aqueous solutions by using iron-modified corn straw biochar. Frontiers of Environmental Science & Engineering, 2015, 9(6): 1066–1075
31. Wang L, Zhang J, Zhao R, Li Y, Li C, Zhang C. Adsorption of Pb(II) on activated carbon prepared from *Polygonum orientale* Linn.: kinetics, isotherms, pH, and ionic strength studies. Bioresource Technology, 2010, 101(15): 5808–5814
32. Ding W C, Peng W L, Zeng X L, Tian X M. Effects of phosphorus concentration on Cr(VI) sorption onto phosphorus-rich sludge biochar. Frontiers of Environmental Science & Engineering, 2014, 8 (3): 379–385
33. Cui L Q, Yan J L, Li L Q, Quan G X, Ding C, Chen T M, Yin C T, Gao J F, Hussain Q. Does biochar alter the speciation of Cd and Pb in aqueous solution? BioResources, 2015, 10(1): 88–104
34. Anwar J, Shafique U, Waheed-uz-Zaman, SalmanM, Dar A, Anwar S. Removal of Pb(II) and Cd(II) from water by adsorption on peels of banana. Bioresource Technology, 2010, 101(6): 1752–1755